

# Solar-Powered/Fuel-Assisted Rankine Cycle Power and Cooling System: Sensitivity Analysis

N. Lior  
Mem. ASME

K. Koai

Department of Mechanical Engineering  
and Applied Mechanics,  
University of Pennsylvania,  
Philadelphia, Pa. 19104

*The subject of this analysis is a solar power/cooling system based on a novel hybrid steam Rankine cycle. Steam is generated by the use of solar energy collected at about 100°C, and it is then superheated to about 600°C in a fossil-fuel-fired superheater. The addition of about 20–26 percent of energy as fuel doubles the power cycle's efficiency as compared to organic fluid Rankine cycles operating at similar collector temperatures. A sensitivity analysis of the system's performance to the size and type of its components was performed by a transient (hourly) computer simulation over the month of August in two representative climatic regions (Washington, D.C. and Phoenix, Ariz.), and led to the description of a system configuration which provides optimal energy performance. The newly designed turbine's predicted efficiency is seen to be essentially invariant with system configuration, and has a monthly average value of about 73 percent.*

## 1 Introduction

Most of the low-temperature (<150°C) Rankine-cycle concepts and systems use organic working fluids and are powered by solar energy alone (cf. reviews in [1–5]). In addition to other possible problems with the use of organic fluids, their temperature cannot be raised into the superheated region, and the cycle efficiency is therefore limited by their boiling temperature. The concept described here, which has been under study and hardware development at the University of Pennsylvania for a number of years, uses steam as the working fluid in a hybrid solar/fuel-powered Rankine cycle ([1, 5–7]). These analyses have shown that, using solar energy to generate steam at about 100°C, the addition of 20–26 percent of the total energy from fuel to superheat the steam to a practical limit of 600°C, approximately doubles the cycle's efficiency as compared to the organic Rankine cycles which operate at similar solar collector temperatures; from about 9 to about 18 percent. Since this results in the reduction of the required collector area by approximately one-half, this hybrid cycle (named SSPRE: "Solar Steam Powered Rankine Engine") has at present a major economic advantage over others.

The advantages of this cycle stem primarily from the thermodynamic improvement associated with proper temperature-matching of heat sources and sinks. Specifically, solar collectors are used at the low temperature where they are both more efficient and less costly, and combustion that is per-force a high temperature process, is used at the highest temperature of the cycle. Using the same principle, the fuel can be replaced by solar concentrating collectors to supply the smaller fraction of energy required by the cycle. Furthermore,

Contributed by the Solar Energy Division and presented at the ASME Winter Annual Meeting, Phoenix, Ariz., November 14–19, 1982. Paper No. WA/Sol-7. Manuscript received by the Solar Energy Division, June, 1982.

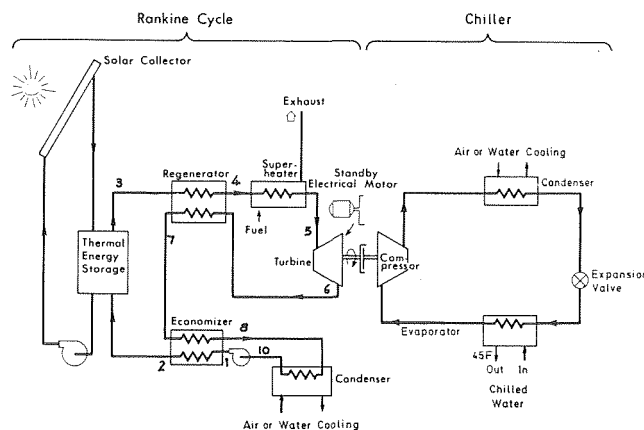


Fig. 1 The Solar-powered/fuel-superheater steam Rankine cycle (SSPRE) driving a vapor-compression chiller  
Typical fluid conditions:

$P_1 = 1.07 \text{ Bar}$ ,	$T_1 = 47^\circ\text{C}$	$P_6 = 0.142 \text{ Bar}$ ,	$T_6 = 336^\circ\text{C}$
	$T_2 = 92^\circ\text{C}$		$T_7 = 162^\circ\text{C}$
$P_3 = 1.06 \text{ Bar}$ ,	$T_3 = 102^\circ\text{C}$		$T_8 = 65^\circ\text{C}$
	$T_4 = 256^\circ\text{C}$	$P_{10} = 0.10 \text{ Bar}$ ,	$T_{10} = 46^\circ\text{C}$

the concept is equally applicable to many low-temperature energy sources, such as geothermal, and waste-heat (cf. [8–10]).

The flow diagram of the cycle considered here, and typical steam conditions, are shown in Fig. 1. Heat is recovered within the cycle by a regenerator and economizer. At present, the cycle's 30 hp output (at design conditions) is produced to drive a commercial open-compressor 25-ton (nominal) chiller. Since commercial low-hp steam turbines would operate in the cycle at a very low efficiency, typically below 50 percent, a

novel 30-hp radial-flow 10-stage turbine with 25 cm diameter counter-rotating rotors using reaction blading was designed and built [11]. Its predicted design efficiency is 75 percent. The thermal storage medium is water, which is allowed to flash for providing steam to the turbine. Consequently, the same fluid (water) is used both in the cycle and for storage.

This paper studies the effect of the size of each of the system's components, and of the type of collectors and condenser cooling on the system's performance, as determined by an hourly computer-simulation over a period of one month (August) at two locations representative for solar cooling: Washington, D.C., and Phoenix, Ariz.

## 2 System Modeling and Analysis

A comprehensive computer program was developed for the transient analysis of the operation and performance of the entire power/cooling system. It is described in detail in a companion paper [12]. The performance of each system component is obtained from its basic configuration and operating conditions. Special attention was given to the parasitic losses, including pumps, fans, and pressure drops in the pipes and heat exchangers, and to off-peak design performance of the components and systems. The program allows the computation of the system performance for practically arbitrary configurations, loads, and climatic regions.

The system sensitivity analysis was performed by varying the size of one component while keeping the others fixed at a "base-case" configuration. The parameters that were varied and their base-case values are shown in Table 1. The superheater<sup>1</sup>, turbine, chiller<sup>2</sup>, and piping (diameter and length) were kept the same throughout the analysis. Evacuated collectors, whose efficiency is characterized by the equation

$$\eta_{coll} = 0.391 - 4.579 \left( \frac{T_i - T_a}{I} \right), \quad (1)$$

where the slope is in (kJ/hr m<sup>2</sup> °C), were used [13]<sup>3</sup>.

Additionally, the potential improvement of the system performance was investigated by replacing the collectors in the base-case configuration by less expensive flat plate collectors which have a higher peak efficiency:

$$\eta_{coll} = 0.78 - 14.19 \left( \frac{T_i - T_a}{I} \right), \quad (2)$$

(in the same units)<sup>4</sup>, and by replacing the air-cooled condenser by a water-cooled one where the condensation temperature is equal to the ambient air dry-bulb temperature. Three cases were investigated here, with the following configurations:

- Case 1: The "base-case" evacuated-tube collector (equation (1)) with a water-cooled power cycle condenser.
- Case 2: Higher-efficiency flat plate collector (equation (2)), with the "base-case" air-cooled power cycle condenser.
- Case 3: Higher efficiency flat plate collector with a water-cooled power cycle condenser.

All the system and component performance evaluation criteria shown in the following are the integrated values of the hourly computed results over the month of August, based on hourly cooling load, weather, and insolation data obtained from [14]. The performance results are examined here in four groups: (1) energy fractions, (2) effectiveness and efficiencies of components, (3) energy quantities and fuel consumption, and (4) cycle efficiency, overall system *COP*, and resource energy saving. These parameters are defined in the following.

<sup>1</sup> Gas-fired, total heat transfer area = 5 m<sup>2</sup>.

<sup>2</sup> Trane Model I-CCOA-025-F with CAUA-250 air-cooled condenser.

<sup>3</sup> Sun Master DEC8A. It is noteworthy that their incidence angle modifier is larger than unity.

<sup>4</sup> These characterize a commercial Ametek collector, but the incidence angle modifier was assumed to be unity.

## Nomenclature

$A$	= area
$h$	= enthalpy
$I$	= insolation, kJ/m <sup>2</sup> hr
$m$	= mass
$P$	= pressure
$RC$	= Rankine cycle
$RE$	= resource energy
$t$	= time
$T$	= temperature
$TFUEL$	= fuel mass flow rate to superheater, kg natural gas
$THFUEL$	= total heat value of fuel supplied to superheater, m <sub>t</sub> (L.H.V.), kJ
$TQCON$	= heat transfer in condenser, m <sub>s</sub> (h <sub>8</sub> - h <sub>10</sub> ), kJ
$TQEC$	= heat transfer in economizer, m <sub>s</sub> (h <sub>7</sub> - h <sub>8</sub> ), kJ
$TQREG$	= heat transfer in regenerator, m <sub>s</sub> (h <sub>6</sub> - h <sub>7</sub> ), kJ
$TQSUP$	= heat transferred to steam in superheater, m <sub>s</sub> (h <sub>5</sub> - h <sub>4</sub> ), kJ
$TRAD$	= solar radiation flux incident on the collector surface, kJ
$TYAUX$	= Rankine cycle parasitic energy (kJ), containing the energy consumption by two pumps (one in collector loop, the other in Rankine loop) and two fans (one in superheater, the other in condenser)
$TYCHIL$	= energy consumption by the condenser fan in the chiller, kJ
$TYMOT$	= back-up electric motor power, kJ

$TYPOWER$	= turbine power output, kJ
$TYPUMP$	= power demand by Rankine cycle pump, kJ
$TY SOL$	= net solar energy gain by the water in the collector, kJ
$TYTANK$	= energy supplied to cycle from storage tank, m <sub>s</sub> (h <sub>3</sub> - h <sub>2</sub> ), kJ
$V$	= volume of water used as thermal storage, m <sup>3</sup>

## Greek

$\epsilon$	= effectiveness
$\eta$	= efficiency
$\eta_e$	= electric energy generation and transmission efficiency (=0.3)

## Subscripts

$a$	= ambient
$coll$	= solar collector
$cond$	= condenser
$ec$	= economizer
$f$	= fuel (gas)
$i$	= inlet to solar collector
$motor$	= electric motor
$reg$	= regenerator
$s$	= steam
$sup$	= superheater

## Superscripts

*	= design conditions
---	---------------------

**Table 1 Parameters for the sensitivity analysis**

Varied parameters	Base-case value	Analysis made for:
Solar collector area, $A_{coll}$	200 m <sup>2</sup>	(1/2, 1, 1½) $A_{coll}$
Thermal storage (water) volume, $V$	37 m <sup>3</sup>	(1/2, 1, 1½) $V$
Regenerator heat transfer area, $A_{reg}$	3.72 m <sup>2</sup>	(1/4, 1, 4) $A_{reg}$
Economizer heat transfer area*, $A_{ec}$	2 m <sup>2</sup>	(1/4, 1, 4) $A_{ec}$
Air-cooled condenser heat transfer area*, $A_{con}$	31.8 m <sup>2</sup>	(3/4, 1, 2) $A_{con}$

\*External area of tubes (excluding the fins)

**(1) The Energy Fractions<sup>5</sup>:**

Solar Energy:  $ZSOL = TYSOL/SOTIN$  (3)

where  $SOTIN$  is the total resource energy used:

$SOTIN = TYSOL + THFUEL + E/\eta_e$  (4)

and  $E$  is total electric energy used:

$E = TYAUX + TYCHIL + TYMOT$  (5)

Fuel energy:  $ZFUEL = THFUEL/SOTIN$  (6)

Electric energy:  $ZE = \frac{E}{\eta_e} / SOTIN$  (7)

Further,  $ZE$  can be split into

RC parasitic:  $Z AUX = \frac{TYAUX}{\eta_e} / SOTIN$  (8)

Chiller parasitic:  $ZCHIL = \frac{TYCHIL}{\eta_e} / SOTIN$  (9)

Back-up motor:  $ZMOT = \frac{TYMOT}{\eta_e} / SOTIN$  (10)

The percentile contribution of the Rankine engine:

In terms of the total cooling load:

$$\%CL = \frac{\left\{ \begin{array}{l} \text{Total cooling load handled by} \\ \text{the Rankine engine} \end{array} \right\}}{\text{Total cooling load of the building}} = \frac{RLOAD}{THLOAD} \quad (11)$$

In terms of total power demand by the compressor:

$$\%RC = \frac{\text{Total power supplied by the turbine}}{\text{Total power demand by the compressor}} = \frac{TYPOWER}{TYPOWER + TYMOT} \quad (12)$$

**(2) Effectiveness and Efficiencies:**

Collector:

$\bar{\eta}_{coll} = TYSOL/TRAD$  (13)

**(3) Energy Quantities and Fuel Consumption:**

The Electric Energy Saving:

For an economic analysis, which compares the energy cost of an electrically driven chiller with that operated by the *SSPRE* system, only the electric energy saving (*EES*) needs to be evaluated against the fuel consumption in the superheater (*THFUEL*).

$$EES = \left[ \begin{array}{l} \text{Total electric energy} \\ \text{used by motor-driven} \\ \text{chiller system} \end{array} \right] - \left[ \begin{array}{l} \text{Total electric energy} \\ \text{used by } SSPRE \\ \text{system} \end{array} \right] = \left\{ \frac{TYPOWER + TYMOT + TYCHIL}{\eta_{motor}} \right\} - \left\{ \frac{TYMOT + TYCHIL + TYAUX}{\eta_{motor}} \right\} = \frac{TYPOWER - TYAUX}{\eta_{motor}} \quad (14)$$

**(4) Cycle Efficiency, Overall System COP, and Resource Energy Saving:**

Thermal efficiency of the Rankine cycle:

$$ZRANK = \frac{\text{Turbine work output}}{\text{Net energy gain in Rankine cycle}} = \frac{TYPOWER}{TQSUP + TYTANK + TYPUMP} = \frac{\int \dot{m}_s (h_5 - h_6) dt}{\int \dot{m}_s [(h_5 - h_4) + (h_3 - h_2) + (h_1 - h_{10})] dt} \quad (15)$$

Overall Rankine cycle efficiency:

$$OZRANK = \frac{\text{Turbine work output}}{\left\{ \begin{array}{l} \text{Total energy input} \\ \text{including parasitic energy} \end{array} \right\}} = \frac{TYPOWER}{TYTANK + THFUEL + TYAUX} \quad (16)$$

**(5) Coefficients of Performance (Several Definitions are Used, Because of the Mix of Energy Inputs):**

Overall system *COP* based on total energy input including all parasitic energy:

$$OCOPP = \frac{\text{Total cooling load}}{\text{Total energy input}} = \frac{THLOAD}{TYSOL + THFUEL + TYAUX + TYCHIL + TYMOT} \quad (17)$$

Overall system *COP* based on resource energy input:

$$OCOPR = \frac{\text{Total cooling load (THLOAD)}}{\text{Total resource energy input (SOTIN)}} = \frac{THLOAD}{TYSOL + THFUEL + (TYAUX + TYCHIL + TYMOT)/\eta_e} \quad (18)$$

<sup>5</sup>Terms undefined in the text are defined in the Nomenclature.

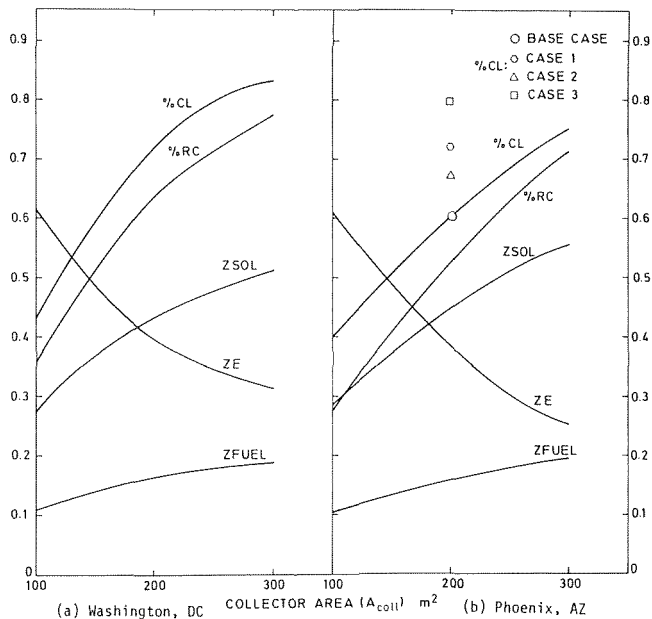


Fig. 2 The monthly energy fractions (solar, fuel, electricity), percent of contribution of Rankine engine to total power demand (% RC), and total cooling load (% CL), as a function of collector area, August

Overall system COP based on total energy conversion excluding all parasitic energy:

$$OCOPS = \frac{\text{Total cooling load}}{\text{Total net energy conversion}} = \frac{THLOAD}{TYTANK + TQSUP + TYPUMP + TYMOT} \quad (19)$$

Overall system COP based on total thermal energy input:

$$OCOPT = \frac{\text{Cooling load handled by Rankine engine}}{\text{Total thermal energy input}} = \frac{RLOAD}{TYTANK + TQSUP} \quad (20)$$

The Percentile Resource Energy Saving:

Here, the total energy saving is evaluated as compared with the same chiller driven entirely by an electric motor. Normalized by the total energy consumption of the electric chiller system, the percentile resource energy saving is computed as follows:

$$ZSAV = (100\%) \frac{\left\{ \frac{TYPOWER + TYMOT + TYCHIL}{0.3\eta_{motor}} \right\} - \left\{ \frac{TYMOT + TYCHIL + TYAUX}{0.3\eta_{motor}} + THFUEL \right\}}{\left\{ \frac{TYPOWER + TYMOT + TYCHIL}{0.3\eta_{motor}} \right\}} = (100\%) \frac{TYPOWER - TYAUX - 0.3\eta_{motor} THFUEL}{TYPOWER + TYMOT + TYCHIL} \quad (21)$$

### 3 Results of the Sensitivity Analysis

**3.1 The Energy Fractions (Figs. 2-4).** The contribution of the Rankine engine to the compressor's power demand (%RC) and toward satisfying the cooling load (%CL) have very similar trends, the difference between them arising from the fact that the cooling capacity does not depend linearly on the power demand. As the collector area increases, (%RC), (%CL), and the solar energy fraction ZSOL increase as expected (Fig. 2). Consequently, the fuel energy fraction ZFUEL increases too, and the backup electric motor is used less, resulting in a proportionate decrease in the electric

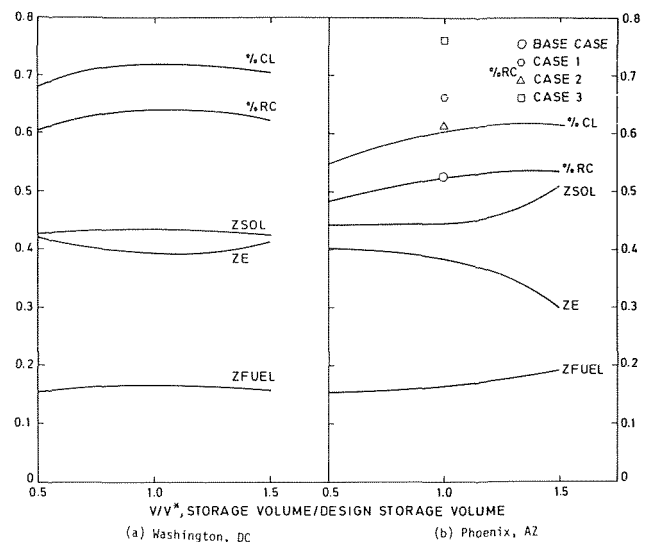


Fig. 3 Monthly energy fractions (solar, fuel, electricity), percent of contribution of Rankine engine to total power demand (% RC), and total cooling load (% CL), as a function of storage volume, August

energy fraction ZE. The base values for (%RC) are 64.1 percent for Washington, and 52.5% for Phoenix, but Phoenix has a higher total power demand and a curve with a steeper slope than Washington. (%RC) can, therefore, be improved in Phoenix by adding more collector area, although 10 percent of the solar energy collected was found to be discarded by the relief valve in the 300 m<sup>2</sup> case (versus 1.9 percent in the base case) because of periods when the storage temperature exceeded 130°C. The (%RC) curve for Washington shows a change of slope around the design area (200 m<sup>2</sup>). Beyond this value (%RC) increases with the area at a lower rate. The energy being discarded there is almost negligible (0.17 percent maximum) in all cases.

As the volume of water in the thermal storage tank increases, the temperature decreases. This creates two opposing effects on (%RC), (%CL), and ZSOL: the collector efficiency increases, but the Rankine cycle efficiency decreases. As a result, a maximum in these values is seen for V/V\* ≈ 1 in Washington, and an approach to a maximum at V/V\* ≈ 1.5 in Phoenix, where the amount of collected energy is higher (Fig. 3). As expected, ZFUEL increases, and ZE decreases, with ZSOL.

The size of the heat transfer area of the regenerator affects the amount of fuel needed in the superheater, the amount of

electricity needed for the condenser fans (the regenerator is also a desuperheater upstream of the condenser), and the steam pressure drop in it. Consequently, as seen in Fig. 4, a system with a small regenerator (say, one-fourth of the design) needs more fuel (12.3 percent over the base value) and electric energy (19.8 percent over the base value) in Washington, which sometimes causes negative value of resource energy saving. In these cases the program's control strategy stops the Rankine engine, and thus the monthly (%RC) is lower. On the other hand, a system with a large regenerator (say, four times the design size) would require higher pressure steam from the storage due to the larger

pressure drop. In Phoenix the pressure drop was found to be around 6.5 percent above the base value. This increased the demand temperature of the storage tank and caused the (%RC) to drop. Therefore, in all, the fraction of the compressor demand supplied by the Rankine engine (%RC) exhibits a maximum in the range of regenerator areas investigated, at  $A_{reg}/A_{reg}^* \approx 1.5$ . As the relative amount of fuel supplied, ZFUEL, decreases with increasing  $A_{reg}/A_{reg}^*$ , the relative solar energy input, ZSOL, increases. ZE, the electrical energy input fraction, has a minimum corresponding to the maximum in (%RC) and (%CL).

The economizer serves a function very similar to that of the regenerator, and the effect on system performance of its heat transfer area thus has similar trends, but of a smaller magnitude, because the economizer recovers typically less than half of the energy recovered in the regenerator. Asymptotic performance values are attained at  $A_{ec}/A_{ec}^* = 1$ . Best performance for the condenser is observed at

$A_{cond}/A_{cond}^* \approx 1.25$ . Below that value, the performance drops rapidly due to severe increase in required cooling fan power.

Figures 2-4 also show the improved performance of the system attained by using higher efficiency collectors and a water-cooled power-cycle condenser. Typically, the smallest improvement is obtained by using the higher efficiency collector alone (Case 1), and the largest when these collectors and a water-cooled condenser are used.

**3.2 Effectiveness and Efficiencies (Figs. 5-7).** Since the ambient temperature and insolation at each location remain the same as the sensitivity analysis parameter is varied, collector efficiency ( $\eta_{coll}$ ) depends only on the temperature of the water at its inlet. This temperature is equal to that of the water in the thermal storage tank. As shown in Fig. 5, ( $\eta_{coll}$ ), which ranges from 0.248 to 0.305, decreases therefore with the collector area in both locations since the storage water temperature (base value: 110°C for 200 m<sup>2</sup>) rises (to 120°C for the 300 m<sup>2</sup> case). The slope  $d(\eta_{coll})/dA_{coll}$  in Washington is<sup>6</sup> 0.032/100 m<sup>2</sup> for  $A_{coll}/A_{coll}^* \geq 1$ , and 0.011/100 m<sup>2</sup> for  $A_{coll}/A_{coll}^* < 1$ . The slope  $d(\eta_{coll})/dA_{coll}$  in Phoenix is 0.01/100 m<sup>2</sup> for the whole range investigated.

The volume of water used as thermal storage affects the storage temperature and thus the collector efficiency. It can be observed in Fig. 6 that ( $\eta_{coll}$ ) in Washington goes through a maximum at around the design volume: small storage volume results in higher water temperatures, and a large volume has lower (%RC) and steam generation rates, resulting again in higher temperatures. In Phoenix,  $\eta_{coll}$  rises modestly with volume, due to the gradual lowering of water temperature.

As a function of regenerator area, ( $\eta_{coll}$ ) approaches the asymptotic value if the areas exceed the design value. Below the design value, the collector efficiency declines because the fan power for the condenser increases as the regenerator area decreases, causing unacceptable or negative energy saving conditions which allow the temperature of the water in the tank to rise (Fig. 7). Similar trends for ( $\eta_{coll}$ ) as a function of the economizer and condenser areas are found for the same reason.

It is noteworthy that the efficiency of the turbine ( $\eta_t$ ), evaluated over the entire month, is essentially unaffected by

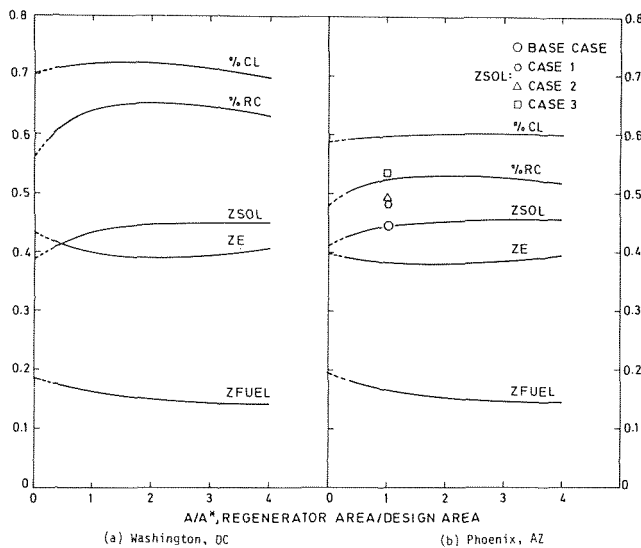


**Fig. 4** Monthly energy fractions (solar, fuel, electricity), percent of contribution of Rankine engine to total power demand (%RC), and total cooling load (%CL), as a function of regenerator area, August

<sup>6</sup>The values represent the decrease in the magnitude of  $\eta_{coll}$ .

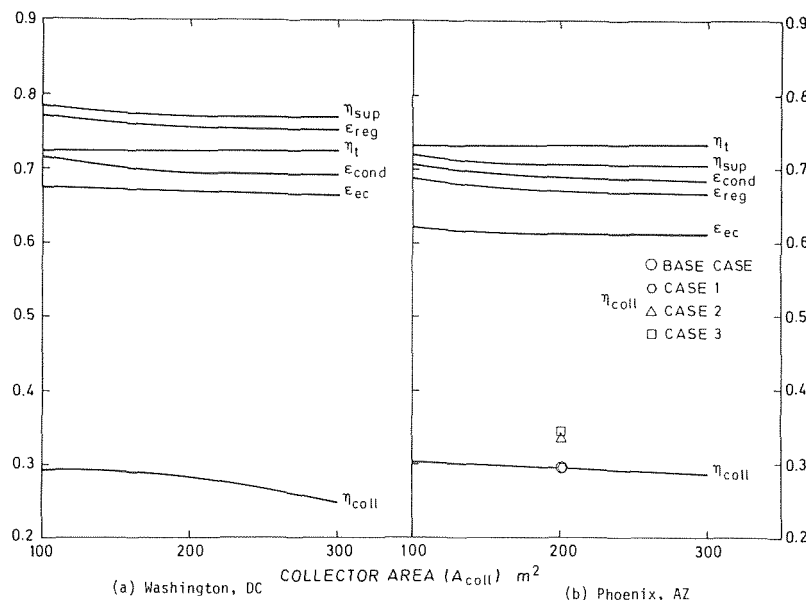


**Fig. 5** Monthly effectiveness and efficiencies as a function of collector area, August

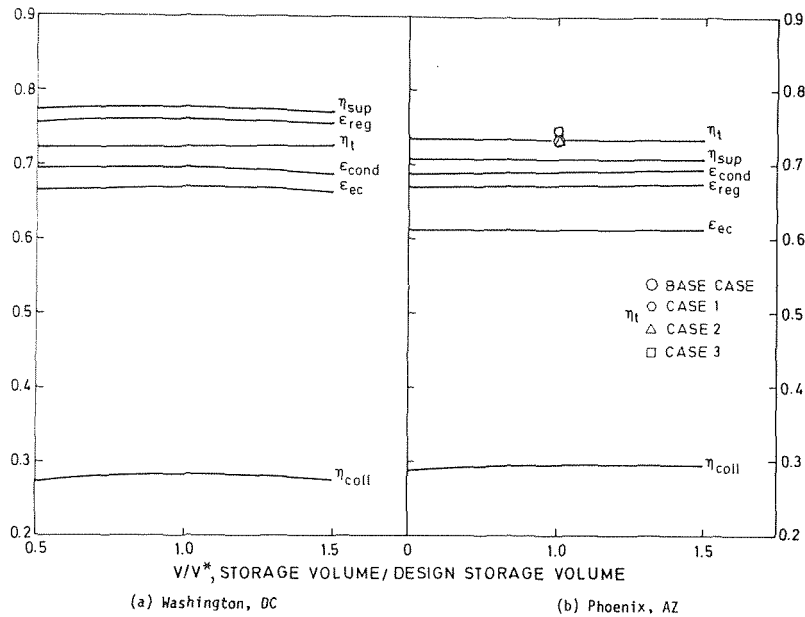


Fig. 6 Monthly effectiveness and efficiencies as a function of storage volume, August

the changes in the system configuration. It is maintained at 0.724 in Washington and at 0.733 in Phoenix. This reflects the excellent off-design performance characteristics implemented into the turbine design, which predicts an efficiency of 0.75 at design conditions [11].

Other efficiencies and effectiveness vary little with the change of parameters. As expected, the effectiveness of the heat exchangers increases with their heat transfer area at a diminishing rate. It can also be seen in Fig. 7 that the effectiveness of the condenser ( $\epsilon_{cond}$ ) and economizer ( $\epsilon_{ec}$ ) decrease to an asymptotic value as the regenerator area increases, since a larger regenerator leaves less heat to be transferred in the economizer and condenser.

**3.3 Energy Quantities and Fuel Consumption (Figs. 8-10).** As seen in Fig. 8, the total energy gain by the collectors (*TY SOL*) increases with the collector area ( $A_{coll}$ ), but not always linearly, since the collector efficiency  $\eta_{coll}$  decreases (see 3.2) as shown in Fig. 7. On average, the slope  $d(TYSOL)/dA_{coll} = (0.12) 10^6 \text{ kJ/m}^2/\text{month}$  in Washington, and  $(0.22) 10^6 \text{ kJ/m}^2/\text{month}$  in Phoenix.

The difference between total energy gain by the collectors (*TY SOL*) and the actual extraction of heat from the storage tank (*TY TANK*) is due to three factors: the heat loss from the tank to the ambient, the heat discarded by the relief valve when the tank temperature exceeds  $130^\circ\text{C}$ , and the internal energy change of the tank water, integrated over the period of operation. The limits of collector area at which energy starts to be discarded can be seen in Fig. 8.

The total Rankine cycle parasitic energy (*TY AUX*), which is constrained by the fact that the power cycle is not operated unless positive resource savings can be materialized, is rather small relative to the other energy quantities. It increases mildly with collector area, due to the increase in  $(\%RC)$  (Figs. 2 and 8) and decreases with regenerator area (Fig. 10), since the fan power demand in the condenser decreases.

The total fuel consumption (*TFUEL*) increases with the collector area ( $A_{coll}$ ) in both locations due to the increasing contribution of the Rankine engine  $(\%RC)$  as discussed in Section 3.1. For similar reasons, a maximum is found for the fuel consumption (*TFUEL*) at  $V/V^* \approx 1$  in Washington, whereas *TFUEL* increases monotonically with the storage volume in Phoenix.

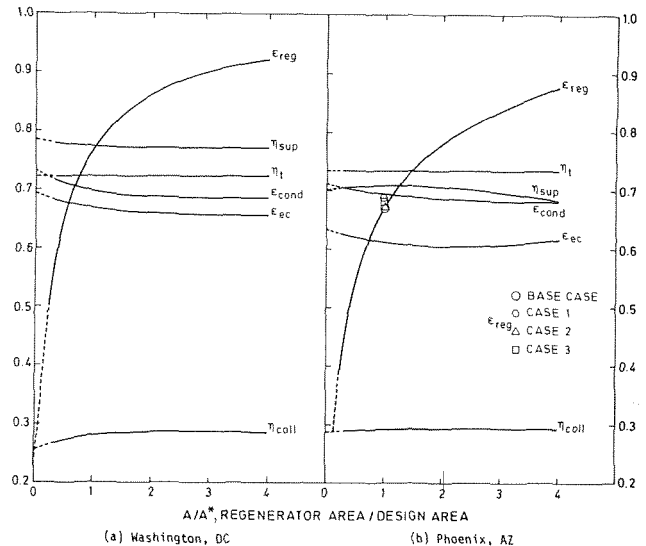


Fig. 7 Monthly effectiveness and efficiencies as a function of regenerator area, August

As expected, the fuel consumption (*TFUEL*) decreases with the regenerator area, since more heat is recovered from the turbine exhaust steam, and thus superheating fuel can be saved (Fig. 10). The slope  $d(TFUEL)/dA_{reg}$ , which is important for the economic evaluation of regenerator area, changes from  $2.355 \text{ kg/m}^2$  (in Washington) and  $5.464 \text{ kg/m}^2$  (in Phoenix) for  $0.25 \leq A/A^* \leq 1$ , to almost zero for  $A/A^* \geq 3.2$  in Washington, and  $A/A^* \geq 2.5$  in Phoenix. The asymptotic limits of fuel consumption are  $200 \text{ kg/month}$  in Washington, and  $300 \text{ kg/month}$  in Phoenix, when  $A_{reg}/A_{reg}^* > 2$ .

The electric energy saving (*EES*) becomes larger with collector area (Fig. 8), but with a decreasing slope, which is particularly pronounced for Washington. This reflects the increasingly larger parasitic losses when the system configuration is maintained constant and only the collector area is enlarged. Again, similar to the case for  $(\%RC)$  (Fig. 2), *EES* has a maximum: at  $V/V^* \approx 0.9$  for Washington, and  $\sim$

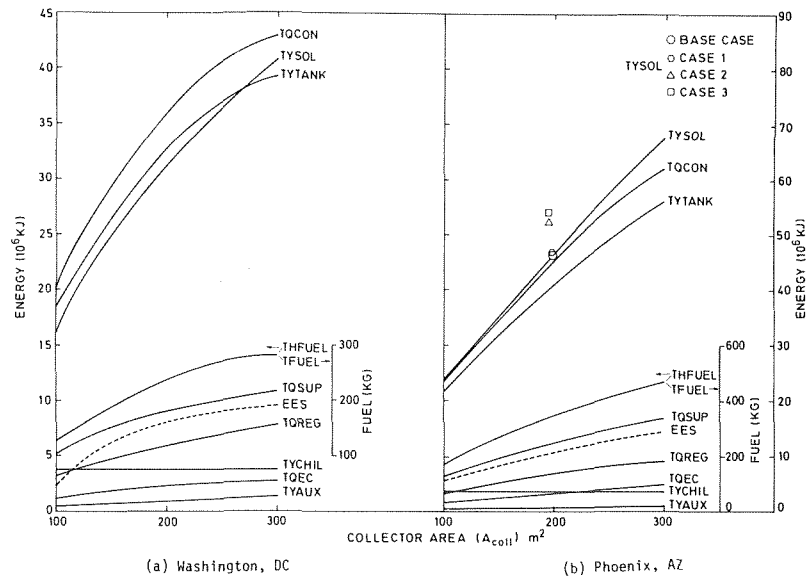


Fig. 8 Monthly energy and fuel consumption as a function of collector area, August

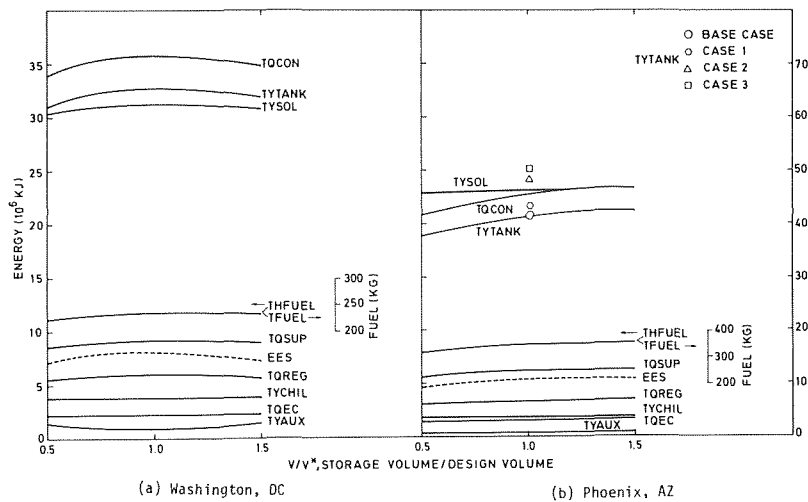


Fig. 9 Monthly energy and fuel consumption as a function of storage volume, August

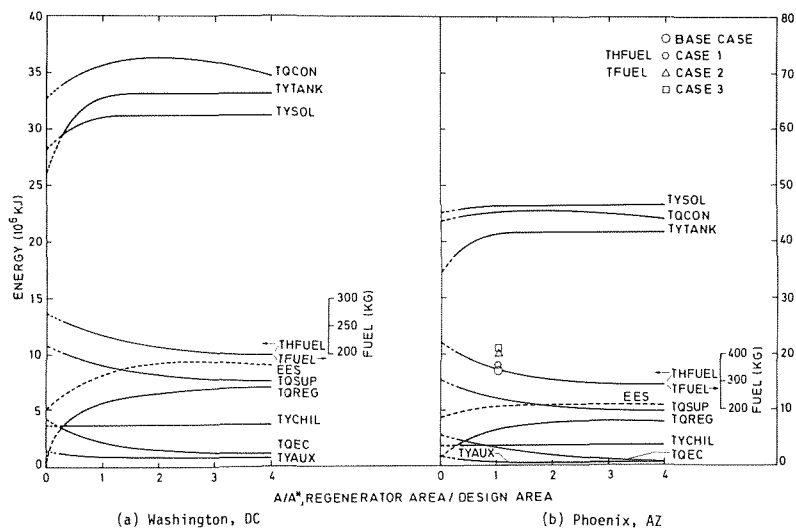


Fig. 10 Monthly energy and fuel consumption as a function of regenerator area, August

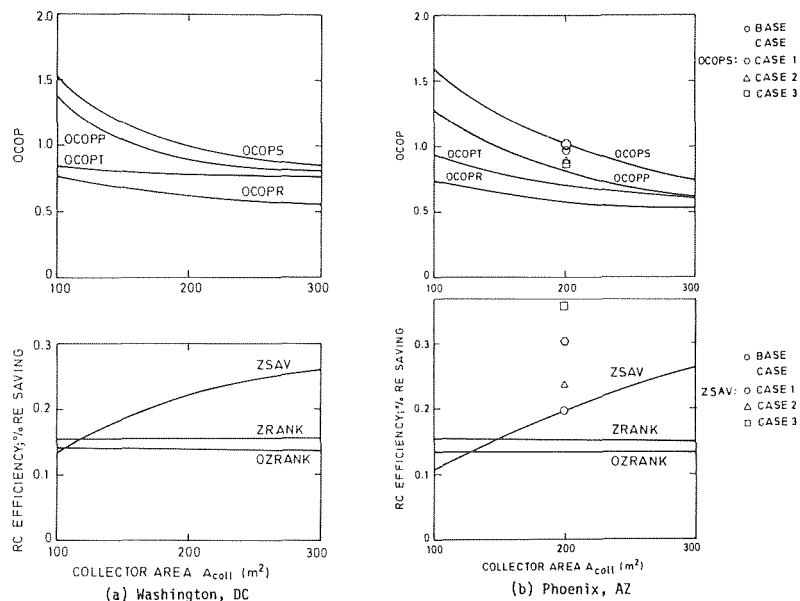


Fig. 11 Monthly percent of resource energy saving, cycle efficiency and COP, as a function of collector area, August

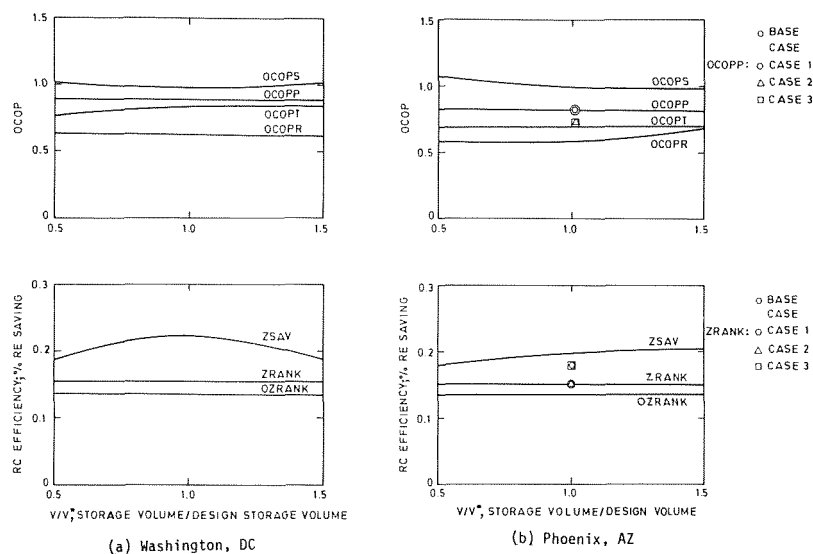


Fig. 12 Monthly percent of resource energy saving, cycle efficiency and COP, as a function of storage volume, August

1.35 for Phoenix (Fig. 9). A maximum is similarly observed for  $A_{reg}/A_{reg}^* \approx 2.2$  in Washington and  $\sim 2.1$  in Phoenix.

**3.4 Cycle Efficiency, Overall System COP, and Resource Energy Saving, (Figs. 11–13).** The overall system COP based on total net energy conversion, (OCOPS), as defined in equation (19), decreases with the collector area in both locations since the solar power conversion efficiency is lower than that of the electric power, and thus more energy is consumed by a system with the larger collector. The base values of (OCOPS) are 1.0 in Washington and Phoenix. (OCOPS) tends to approach an asymptotic value for  $A_{coll}/A_{coll}^* > 1$ , due to the trend of (%RC) as shown in Fig. 2.

In Washington, the overall system COP based on the net total thermal energy input, (OCOPT), as defined in equation (20), remains nearly independent of the collector area. In Phoenix it decreases with the collector area.

The other definitions of overall system COP, i.e., (OCOPP) and (OCOPR), as defined in equations (17) and (18), are also shown in Fig. 11. In general, (OCOPP) follows

the trend of (OCOPS), but is somewhat lower since the efficiency of superheater, and parasitic energy of the chiller are included.

The variations of the overall system COP as function of other component geometries are minor, as shown in Figs. 12 and 13.

The Rankine cycle thermal efficiency (ZRANK) and overall efficiency (OZRANK) are almost constant in all cases (base value: ZRANK=0.16, OZRANK=0.14 in Washington; ZRANK=0.15, OZRANK=0.14 in Phoenix), except for the cases having heat exchange areas below the design value, where (ZRANK) and (OZRANK) fall as expected (Figs. 11–13).

The percent of resource energy saving (ZSAV) over electric chillers as defined in equation (21) increases with the collector area substantially. Like the trend of (%RC) as discussed in Section 3.1, ZSAV is closer to being linearly proportional to the area in Phoenix than in Washington. The base values of ZSAV are 0.20 in Phoenix and 0.23 in Washington. The slope  $d(ZSAV)/d(A_{coll})=0.0785/100$  m<sup>2</sup> in Phoenix. The ZSAV

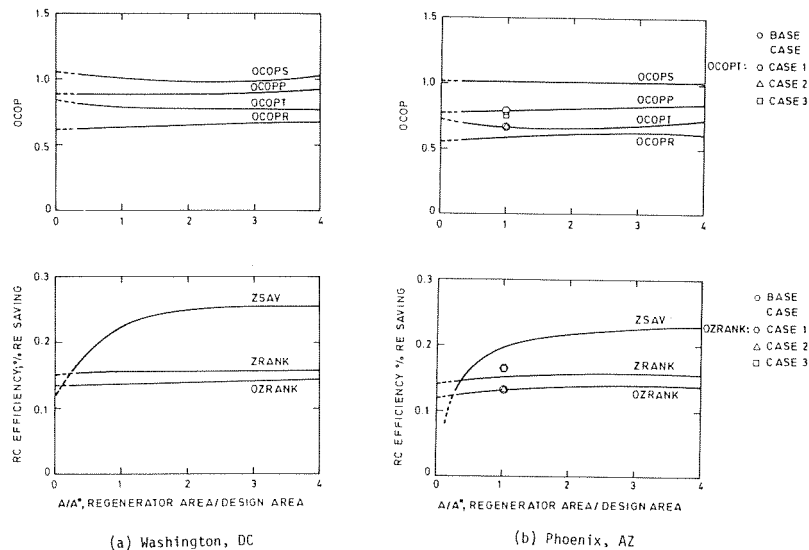


Fig. 13 Monthly percent of resource energy saving, cycle efficiency and COP, as a function of regenerator area, August

Table 2 System configuration for optimal performance (results for August)

	Washington, D.C.	Phoenix Ariz.
Collector area ratio $A_{coll}/A_{coll}^*$	1.2	1.5-1.6
Thermal storage water volume ratio, $V/V^*$	0.9-1.0	1.4
Regenerator area ratio $A_{reg}/A_{reg}^*$	1.5	1.6
Economizer area ratio $A_{ec}/A_{ec}^*$	1.0	1.0
Condenser area ratio $A_{cond}/A_{cond}^*$	1.2	1.1

curve for Washington shows a change of slope at around the design area (200 m<sup>2</sup>). Beyond this value, ZSAV approaches an asymptotic value (approximately 0.27). In Phoenix, however, such asymptotic behavior is not found in the studied range. Therefore, continuous improvement of ZSAV can be made by increasing the collector area.

A resemblance between the trend of ZSAV and (%RC) (Fig. 3 versus Fig. 12) can be found in their variation as function of the storage volume. In Washington, ZSAV has a maximum at  $V/V^* = 1$ , whereas in Phoenix, ZSAV still increases with the storage volume beyond the design value. The latter occurs because the Rankine engine power output (TYPOWER) increases more substantially than TYAUX and THFUEL (equation (21)) as storage volume is increased. In Washington, however, (TYPOWER) has a maximum at the design point.

As a function of regenerator and economizer and condenser area, asymptotic values for ZSAV are found for areas above the design value (Fig. 13).

Figure 11 shows the remarkable improvements that can be obtained in resource energy savings by using higher efficiency collectors and/or a water cooled condenser: an 85.5 percent improvement in ZSAV is obtained for Case 3. The water-cooled condenser alone (Case 2) improves the performance by 56.2 percent. Similarly, Fig. 13 shows a 23.3 percent increase in OZRANK. As shown in [12], a feasible reduction in the chiller-condenser's fan-power, or the use of a water-cooled condenser, and the use of a commercially available chiller with a higher COP, would increase the overall COP (OCOPP) from the base-case value of 0.85 to 1.35.

#### 4 Summary and Major Conclusions

1 The sensitivity analysis of the hybrid solar-powered/fuel-assisted power/cooling system performance to the size and

type of components used, provides the basis for its technological optimization.

2 Less than 20 percent of the input energy is fuel, to superheat steam generated by solar energy at the low temperature of around 100°C, and this approximately doubles the Rankine cycle efficiency. This results in an overall resource energy saving of 20-25 percent for the base-case system analyzed.

3 A system configuration that provides optimal energy performance is described in Table 2 for the two sites.

4 The predicted efficiency of the novel turbine designed for this project is essentially invariant with system configuration, (72.4 percent in Washington, and 73.3 percent in Phoenix), demonstrating excellent off-design performance.

5 Compared to the base-case configuration, water-cooling of the power-cycle condenser and the use of flat-plate collectors of higher efficiency result in marked improvement of the performance: The Rankine cycle efficiency increases by up to 23.3 percent (13.4-16.5 percent), the electric energy savings increase by up to 56.1 percent, and the resource energy savings increase by up to 85.5 percent (from 19.7 percent at base-case to 36.6 percent, and up to a value of 46.4 percent with a 50 percent larger regenerator).

#### 5 Acknowledgment

The authors wish to gratefully acknowledge the contributions of Professor H. Yeh to this work, and the assistance and cooperation of Philadelphia Gear Corporation, The Trane Company, and United Engineers and Constructors, Inc., which were subcontractors to the University of Pennsylvania. This project was supported by the USDOE Office of Solar Heat Technology, Active Research Branch.

## 6 References

- 1 Curran, H. M., "Assessment of Solar-Powered Cooling of Buildings," Hittman Associates, Final Report HIT-600, (NTIS: COO/2522-1), April 1975.
- 2 Lior, N., "Solar Energy and the Steam Rankine Cycle for Driving and Assisting Heat Pumps in Heating and Cooling Modes," *Energy Conversion*, Vol. 16, 1977, pp. 111-123.
- 3 Merriam, R., "Solar Air Conditioning Study," NTIS Document No. AD/A-043-951, 1977.
- 4 Lior, N., Yeh, H., and Zinnes, I., "Solar Cooling Via Vapor Compression Cycles," *Proc. 1980 Annual Meeting, International Solar Energy Society, American Section, Phoenix, Ariz.*, Vol. 3.1, 1980, pp. 210-214.
- 5 Lior, N., "Methods for Improving the Energy Performance of Heat Pumps," presented at the 9th Intersociety Energy Conversion Engineering Conf., San Francisco, Calif., Aug. 1974. (Also University of Pennsylvania MEAM Report No. 74-4, 1974).
- 6 Curran, H. M., and Miller, M., "Evaluation of Solar-Assisted Rankine Cycle Concept for the Cooling of Buildings," *Proc. 10th IECEC*, Paper No. 759203, 1975, pp. 1391-1398.
- 7 Koai, K., Lior, N., and Yeh, H., "Analysis of a Solar-Powered/Fuel-Assisted Rankine Cycle for Cooling," *Proc. 1982 Annual Meeting, American Solar Energy Society*, Houston, Texas, 1982, Part 1, pp. 573-578.
- 8 Martin, C. G., and Swenson, P. F., for Energy Technology, Inc., "Method of Converting Low Grade Heat Energy to Useful Mechanical Power," U.S. Patent No. 3,950,949, 1976.
- 9 DiPippo, R., Khalifa, H. E., Correia, R. J., and Kestin, J., "Fossil Superheating in Geothermal Steam Power Plants," *Proc. 13th IECEC*, Vol. 3, 1978, pp. 1095-1101.
- 10 DiPippo, R., Kestin, J., Avelar, E. M., and Khalifa, H. E., "Compound Hybrid Geothermal-Fossil Power Plants: Thermodynamic Analyses and Site-Specific Applications," ASME Paper No. 80-Pet-83, 1980.
- 11 Kroon, R. P., Meyer, C. A., Lior, N., and Yeh, H., "Design of a 30 HP Solar Steam Powered Turbine," Topical Report DOE/ET/20110-3 (DE82007236) to the USDOE, May 1981.
- 12 Lior, N., and Koai, K., "Solar Powered/Fuel-Assisted Rankine Cycle Power and Cooling System: Simulation Method and Seasonal Performance," *ASME JOURNAL OF SOLAR ENERGY ENGINEERING*, Vol. 106, May 1984.
- 13 Wyle Laboratories, "Indoor Test for Thermal Performance of the Sunmaster Evacuated Tube (Liquid) Solar Collector," DOE/NASA Contractor Report CR-161306, Sept. 1979.
- 14 Leboeuf, C., "Standard Assumptions and Methods of Solar Heating and Cooling Systems Analysis," SERI/TR-351-402, Solar Energy Research Institute, Jan. 1980.